

AD-A117 399

HARRY DIAMOND LABS ADELPHI MD
DESIGN OF MICROSTRIP LINEAR ARRAY ANTENNAS BY COMPUTER. (U)
JUN 82 M CAMPI

F/6 9/5

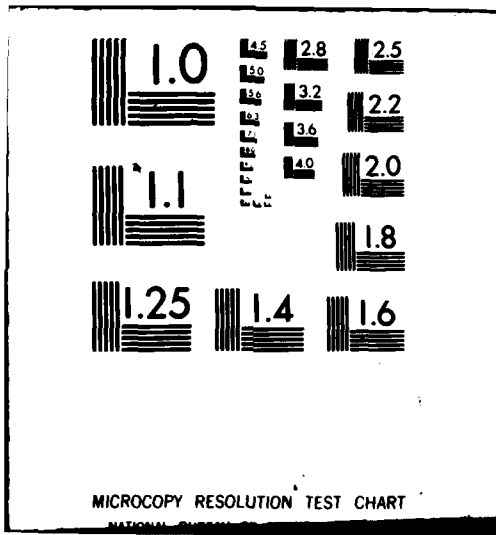
UNCLASSIFIED

NL

1-1
4-1



END
DATE
FILMED
8-8
DTI



MICROCOPY RESOLUTION TEST CHART

NATIONAL BUREAU OF STANDARDS-1963-A

①

18 JUN 1982
~~20 JUN 1982~~

CAMPI

AD A117399

DESIGN OF MICROSTRIP LINEAR ARRAY ANTENNAS
BY COMPUTER

MORRIS CAMPI, PH.D.
U.S. ARMY ELECTRONICS RESEARCH AND DEVELOPMENT COMMAND
HARRY DIAMOND LABORATORIES
ADELPHI, MARYLAND 20783

Introduction

Research in microstrip antenna technology and design is currently being developed to meet the present and future needs of military radar and fuze system requirements. Configured in either single- or multiple-lattice structures, microstrip has the advantages of ease in fabrication, low cost, light weight, and structural conformability. When designed to have either a series or a corporate feed network, the lattices become antenna arrays that can be used for transmitting and receiving signals from microwave through millimeter frequencies into the lower regions of the near-millimeter wave portion of the spectrum. However, the present state of the art is at the same stage of development as existed for waveguide slot array designs in the late 1950's and early 1960's. This stage is a "cut-and-try" period in which an empirical design takes from weeks to months of fabrication and testing before satisfactory results are obtained; even then, one can never be sure of achieving the optimum design to meet the system's specific requirements.

DTIC FILE COPY

→ Today, computer aided design codes can be developed to help antenna engineers in their design of linear or planar array microstrip antennas. This report describes one such code that was developed by using both empirical data and a theoretical model. One major feature of this code is that it allows the designer to vary any one or more of the antenna design parameters and to observe the results, such as changes in the radiation pattern or amplitude distribution displayed at the computer terminal screen. This application provides the tool required by the engineer to determine in a matter of seconds the prime factors affecting his design and to make parametric adjustments or sensitivity studies to help understand and develop his final product. Once a design is established, the engineer is presented with a set of coordinate numbers that can be placed on magnetic or paper tape, which can then be used to fabricate the antenna on printed circuit board without the need for drawings or art-

S DTIC ELECTE D
JUL 20 1982
B

DISTRIBUTION STATEMENT A
Approved for public release;
Distribution Unlimited

82 07 19 294

1

→ cont

CAMPI

over a conducting ground plane separated by a thin layer of dielectric material, where the material thickness is much less than one wavelength. By use of inexpensive printed circuit technology, the patch element is readily fabricated by using etching techniques applied to metal clad dielectric, usually Teflon or Teflon impregnated with fiberglass sandwiched between thin copper plating.

The patch width, W , determines the electrical admittance of the element, and the dimension l (nearly one-half wavelength) determines the frequency at which resonance occurs. The element consists basically of two radiating slots perpendicular to the feed line and separated by a transmission line of very low impedance (1). At resonance, the element is an efficient radiator of electromagnetic energy. The resonant line length of the patch is slightly less than one-half wavelength because of phase modifications due to substrate thickness, fringing field capacitance, and the patch aspect ratio. It is calculated (2) as

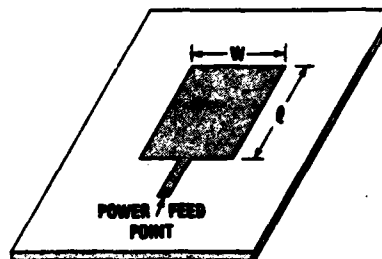


Fig. 1. Geometry of microstrip patch element.

$$l = c / (2f_0 \sqrt{\epsilon_e}) - \delta l \quad (1)$$

where $c = 30$, f_0 is the resonant frequency in gigahertz,

$$\epsilon_e = \frac{\epsilon_d + 1}{2} + \frac{\epsilon_d - 1}{2} \left(1 + \frac{12h}{W}\right)^{-1/2} \quad (2)$$

$$\delta l = 0.412h \frac{(\epsilon_e + 0.3)(W/h + 0.264)}{(\epsilon_e - 0.258)(W/h + 0.8)} \quad (3)$$

ϵ_e is the effective dielectric constant, ϵ_d is the dielectric constant, and h is the dielectric thickness.

The fields radiating from these slots have components parallel to the ground plane, which add in phase to give a maximum radiated field normal to the element. Figure 2 illustrates the geometry of a radiating slot.

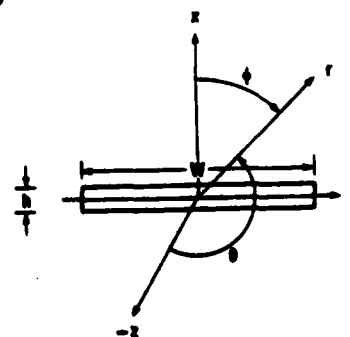


Fig. 2. Geometry of radiating slot.

CAMPI

The total power radiated from each slot is obtained by integrating the real part of the Poynting vector from a single slot over a hemisphere of large radius. It is derived as

$$P = \sqrt{\frac{\epsilon}{\mu}} \frac{V_0^2}{\pi} \int_0^\pi \frac{\sin^2 \left(\frac{\pi W}{\lambda_0} \sin \phi \right)}{\sin^2 \phi} \cos^3 \phi \, d\phi \quad (4)$$

where V_0 is the voltage across the slot of height h , which is very small, that is, $k_0 h \ll 1$, where k is the propagation constant equal to $2\pi/\lambda_0$.

Microstrip Element Conductance

Since rigorous transmission line or two-port parameters are not available for a resonant, radiating microstrip patch, it is modelled as a lumped conductance and a phase delay. The delay is taken into account for the phasing of series-feed arrays; the combined power radiated by the two slots of a patch is the same as that dissipated by the conductance, G , having across it the voltage, V_0 , at the center of the slot; hence, $G = P/V_0^2$ or $G = I/\pi\sqrt{\epsilon/\mu}$, where

$$I = \int_0^\pi \frac{\sin^2 \left(\frac{\pi W}{\lambda_0} \sin \phi \right)}{\sin^2 \phi} \cos^3 \phi \, d\phi \quad (5)$$

The integral, I , is solved by use of computer integration techniques. In the range $0.033 \leq W/\lambda_0 \leq 0.254$, conductance values have been measured and follow the relation (3)

$$G = 0.0162 \left(\frac{W}{\lambda_0} \right)^{1.757} \quad (6)$$

Insertion Phase

Transmission line discontinuities produce phase shifts or delays in the propagation of energy down the transmission line. The impedance mismatch and line-to-patch width aspect ratio at the entrance and exit ports of each microstrip patch produce phase delays to the propagating signal. Most importantly, mode structure and wave number along the longitudinal axis of the microstrip cavity can introduce a large insertion phase shift between input and output ports in addition to the desired phase shift of 180° . This effect does not alter the resonance condition of the patch, but increases the effective phase delay to the following patch in the array and thus changes the composite radiation pattern. For example, if all the patch widths were equal, the resulting constant insertion phase of each patch would rotate the main lobe of the antenna pattern. However, most array designs require element widths of different

CAMPI

sizes, which cause unequal insertion phases to occur and modify the pattern in even less desirable ways.

One method to compensate for the insertion phase is to shorten the transmission line lengths between the elements by an amount Δl such that $\Delta l/\lambda_e = \phi_e/2\pi$, where λ_e is the signal wavelength in the dielectric and ϕ_e is the insertion phase. The effect of the dielectric is to change the wavelength dimension from the free space value, λ_0 , to the dielectric value, λ_e , by the relation $\lambda_e = \lambda_0/\sqrt{\epsilon_r}$. The reduction in length by this method causes the patch separation to have the desired equal electrical path lengths, but unequal physical lengths.

Mutual Coupling

The proximity of one patch element positioned close to another in forming an array will cause coupling of the electric (E-) or magnetic (H-) fields, depending on the patch element plane orientation. A series-feed array aligns the E-fields to be oriented along the array direction. Published literature (4,5) and in-house experiments* provide some data for mutual coupling between two nearly square, resonant patches, one driven through a 50-ohm microstrip line and unterminated and the other one terminated in 50 ohms. At a gap width of $0.1 \lambda_0$, the power received by the passive patch is about 17 dB below the power absorbed by the driven patch, and the received power decreases with increasing separation. These data were tabularized in a subroutine and are used in designing an array; however, the effect is normally negligible.

Theoretical Model

The model for the multielement linear array used in the antenna computer code is represented by a transmission line network with shunt loads as shown in figure 3. Each array element is represented by a normalized shunt admittance, Y_i , that radiates power, P_i . The total admittance of the line to the right of the i th element, seen from this point, is represented by Y_i^+ . Y_i^- is the total admittance looking to the right at the i th location, which includes the i th admittance, so $Y_i^- = Y_i + Y_i^+$. The admittance transformation by a line section of length l is given by

$$Y_i^+ = \frac{Y_{i+1}^- \cosh \gamma l + \sinh \gamma l}{\cosh \gamma l + Y_{i+1}^- \sinh \gamma l} \quad (7)$$

here, $\gamma = \alpha + j\beta$ is the complex propagation constant of the unloaded line, where γ is the complex propagation constant, α is the attenuation constant, and β is the phase constant. The length l includes the

*F. Farrar, Harry Diamond Laboratories.

CAMPI

electrical length of the patch as well as the interconnecting transmission line.

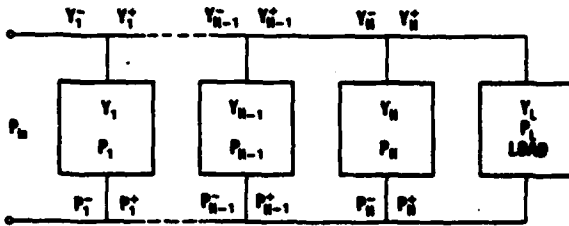


Fig. 3. Equivalent network representation of multi-element array model used for computer aided design.

A single-cell analysis of the array elements is illustrated in figure 4a. P_i^- is the power incident to the i th element. If Γ_i^2 is the power reflection coefficient at the i th element such that $P_{i(\text{reflected})} = \Gamma_i^2 P_i^-$, then the total net transported power at a point to the left of element i is

$$P_{i(\text{total})} = P_i^- - P_{i(\text{reflected})} \tag{8}$$

$$= P_i^- (1 - \Gamma_i^2)$$

and the power transmitted past the element is the difference between that and the power P_i radiated by the element:

$$P_i^+ = P_{i(\text{total})} - P_i \tag{9}$$

$$= P_i^- (1 - \Gamma_i^2) - P_i$$

The patch admittance, Y_i , is actually the aforementioned lumped radiation conductance, G_i (fig. 4b). The radiated power, P_i , may be expressed by G_i and an equivalent element voltage, V_i , as $P_i = |V_i|^2 G_i$. Similarly, the transmitted power is

$$P_i^+ = |V_i|^2 R_e(Y_i^+) \tag{10}$$

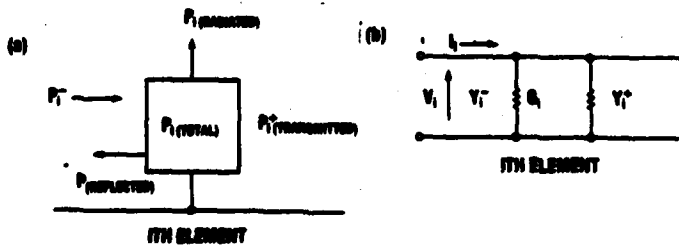


Fig. 4. i th element:
(a) single cell analysis of power distribution and
(b) schematic representation.

CAMPI

Note that a reflection from the following patch, P_{i+1} (reflected), is included in P_i^+ because Y_i^+ according to equation (7) is the precisely transformed input admittance of this patch. The total input conductance is

$$R_e(Y_i^-) = G_1 + R_e(Y_i^+) \quad . \quad (11)$$

With equations (9) to (11), the radiated power can be expressed as

$$P_i(\text{radiated}) = P_i^-(1 - \Gamma_i^2)G_1/R_e(Y_i^-) \quad , \quad (12)$$

where

$$\Gamma_i = \left| \frac{1 - Y_i^-}{1 + Y_i^-} \right| \quad .$$

Equation (12) can be used to determine the power radiated from any element in the array, provided that one other relationship is known. At the first element, P_1 is the input power (usually normalized to 1). The total input admittance is Y_1^- , and G_1 is the first element conductance. To transform the power from the first to the second element, an additional relationship,

$$P_{i+1}^- = P_i^+ e^{-2\alpha l} \quad , \quad (13)$$

needs to be used* so that from equation (9)

$$P_2^- = P_1^+ e^{-2\alpha l} = [P_1^-(1 - \Gamma_1^2) - P_1^+ e^{-2\alpha l}] \quad (14)$$

and

$$P_2 = P_2^-(1 - \Gamma_2^2)G_2/R_e(Y_2^-) \quad . \quad (15)$$

The above equations appear as recursion relations, which are quite useful for generating and analyzing N-element array designs with the aid of a computer. Given the normalized conductor elements, G_1 , the spacial element separation, l , and the propagation coefficients, α and β , the normalized power radiated from each element is determined. However, array designs for antennas usually prescribe the radiated power from each element as input data, and the engineer must determine the element conductances that form the array--in essence, working the problem

*Equation (13) relates the exponential decay of the power from losses as it translates along the transmission line from one element to the next.

CAMPI

backward. This task requires the solution to an implicit equation, that is, having knowledge of the conductance values to determine the conductance values. To solve the task, a computer program was written by using the explicit relations of $P_1 = f(g_1)$ with an optimization subroutine.* This subroutine continuously alters the conductance value of each element until it finds a set of values such that the calculated power best approximates in a least squares sense the prescribed radiated power distribution.

Computer Model

The computer program reported here was developed to provide design data for fabricating a linear series microstrip array antenna. The design is based on information provided by the user as he answers a series of questions that are displayed on the terminal screen.

The program computations normalize impedances or admittances to the line characteristic impedance or admittance as chosen. Distance also is dimensioned by normalizing to the wavelength of interest, as it is measured in the dielectric or free space if so chosen. The element separation need be dimensioned only as decimal parts of a wavelength. Actual design dimensions need not be determined until the antenna design is completed and resonant frequency is assigned.

The program also offers options for considering the effects of (a) reflections due to impedance mismatch at each element, (b) patch directivities due to the broadside gain of each element, (c) insertion phase, and (d) compensation for insertion phase. This capability and the others mentioned provide for a variety of parametric studies toward determining the casual relations of the antenna pattern peculiarities and sensitivity studies important in understanding the effect of manufacturing tolerances.

If the conductance values of the array elements are unknown, they are calculated by the program after the power distribution is entered. Six commonly used power distributions are programmed and are available for use. Other power distributions can be entered manually at the keyboard.

Calculation of Conductances

Equation (12) can be rewritten so that

$$G_1 = \frac{P_1(\text{radiated})}{P_1^-(1 - \Gamma_1^2)} R_e(Y_1^-) \quad (16)$$

*Copyright 1978 by IMSL, Inc.

CAMPI

This equation is not explicit in G_i since Γ_i^2 and Y_i^- also contain G_i . However, an optimum design requires minimum or no reflections ($\Gamma_i^2 \ll 1$) along the array elements resulting from good impedance matching ($R_e Y_i^- \approx 1$). Therefore, as a first estimation of G_i , Γ_i^2 and Y_i^- are removed and the relation $G_i = P_i(\text{radiated})/P_i$ is used. Once the set of G 's is calculated from the given power distribution, the G 's are then used to recalculate the radiated power distribution and the antenna efficiency by use of equation (12). The efficiency of an array used in this report is defined as the ratio of the total power radiated to the power delivered at the input. (Losses include the power absorbed at the termination and the power reflected from each element back to the generator.) For low efficiency design, the power distribution calculated is in fair agreement with the initial power distribution used as input data to the program. Figure 5 plots the initial and given power distributions that were calculated to radiate from the elements. Better fits can be obtained by using the optimization subroutine.

Optimization

An algorithm in the program computes an initial estimate of the required element conductances. However, for most applications of the array code, the resulting low efficiency or undesired distribution of radiated power makes the code somewhat limited or useless. An optimization routine can be used as an option to provide a better or perfect match of the two power distributions. This routine calls on a subroutine that generates the calculated power distribution from the calculated radiated power of each element and compares the distribution with that given as input data. The square of the difference is calculated, and the optimization routine varies the conductance values to minimize this difference. When the calculations are completed, the power calculated to radiate from each element is in very good agreement with the input power data, and the conductance values generated are used for designing the array. Figure 6 shows an example of the results of the optimization routine used for a particular design.

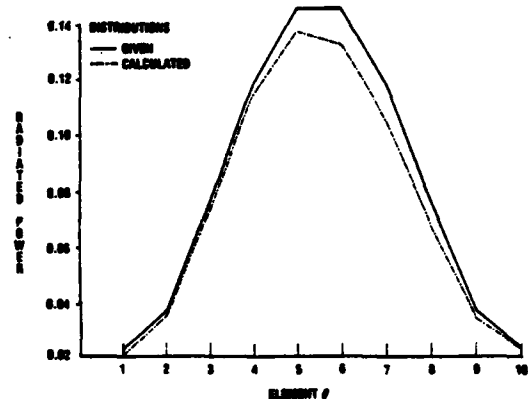


Fig. 5. Initial and given power distributions calculated to radiate from elements.

CAMPI

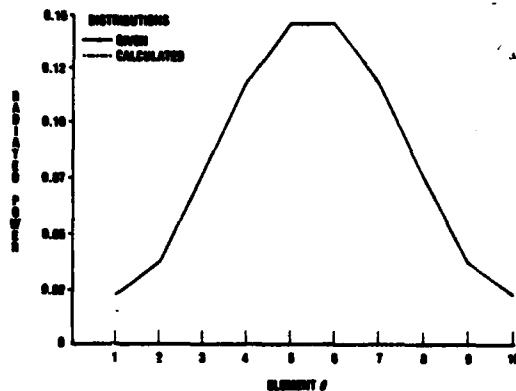


Fig. 6. Results of optimization routine used for particular design.

The antenna radiation pattern from the generated design can be displayed on the terminal screen over any desired angular range for either linear or polar plots.

Power Distribution Subroutines

The power distribution to be radiated over the antenna aperture may be inserted into the program either by use of a terminal keyboard or by use of the following distributions already available in the program as subroutines:

- Uniform
- Tchebyscheff
- Taylor
- Cosine square on pedestal
- Binomial
- $(1 - x^2)^M$ polynomial

The choice of any specific distribution must include tradeoffs among gain, beam width, and side-lobe levels, a choice usually dictated by system requirements. Here, the computer code is particularly useful in displaying the design for each distribution, where comparisons of each feature may be explored with relative ease. However, it is important to have some basic knowledge of the various distributions before attempting a design. The uniform distribution provides for the highest gain at a narrow beam width, but the side lobes are high (-13.2 dB).

The Tchebyscheff and Taylor distributions provide for side-lobe control at some loss to antenna gain. The Tchebyscheff distribution produces the narrowest beam width for a given side-lobe level; however, the side lobes are equal. For many applications, the equal-side-lobe-level pattern may be undesirable. In the Taylor distribution, the side lobes decrease as the angle from the main beam increases, but at the sacrifice of a slightly increased beam width. Both the Tchebyscheff and

CAMPI

Taylor distributions enable the designer to select a desired side-lobe level and to compute the element excitation values in terms of a parameter related to the side-lobe level.

The distribution of cosine square on a pedestal is a truncated distribution in which the ratio of the pedestal height to the distribution peak determines the side-lobe level. The binomial distribution produces no side lobes, but at the expense of low gain and wide beam widths. The polynomial distribution provides for a class of distributions in which further tradeoffs among gain, beam widths, and side lobes can be studied simply by varying the factor m in the polynomial.

The variety in aperture distributions offered by this program should provide for most systems needs. New or unique distributions can be added easily to the existing program as subroutines to expand the scope of this design code.

Antenna Designs

Several linear and planar arrays were designed by using the microstrip computer model. Figure 7 shows a microstrip S-band array that was successfully designed to exhibit the same antenna characteristics (except for polarization) as those derived from the slotted waveguide array. The microstrip array, however, is E-plane polarized along the array direction, and the waveguide array is H-plane polarized. A number of linear arrays were combined by use of a corporate-feed structure to form a planar array as shown in figure 8. Figure 9 shows a polar plot of the antenna radiation pattern for both the E-plane (series-feed direction) and the H-plane (corporate-feed direction) polarizations. The success at designing microstrip antennas at microwave frequencies prompted an array design for use at around 100 GHz. Figure 10 shows the array mounted in a test fixture, and figure 11 shows the linear plot for both the theory and experimental results.

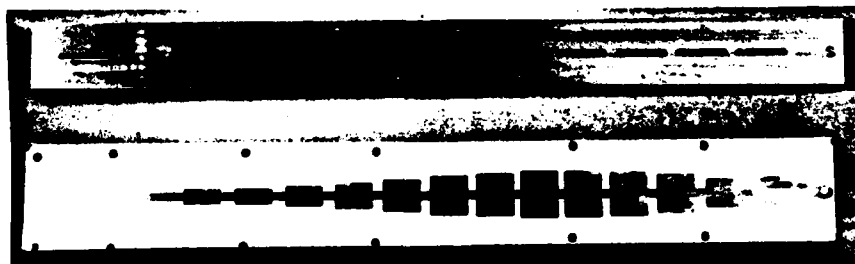


Fig. 7. Microstrip antenna designed to have characteristics similar to those of waveguide array shown above.

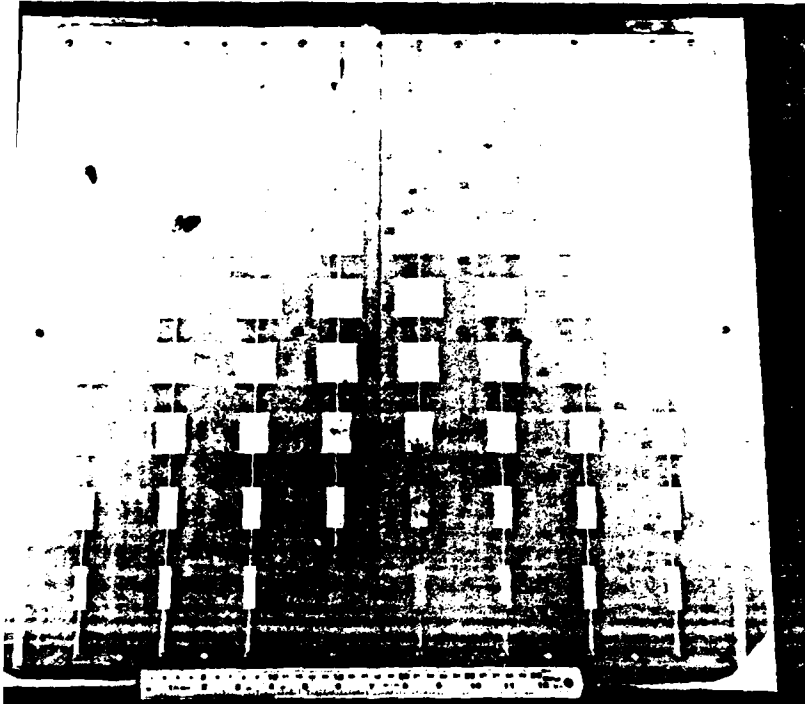


Fig. 8. Microstrip planar array.

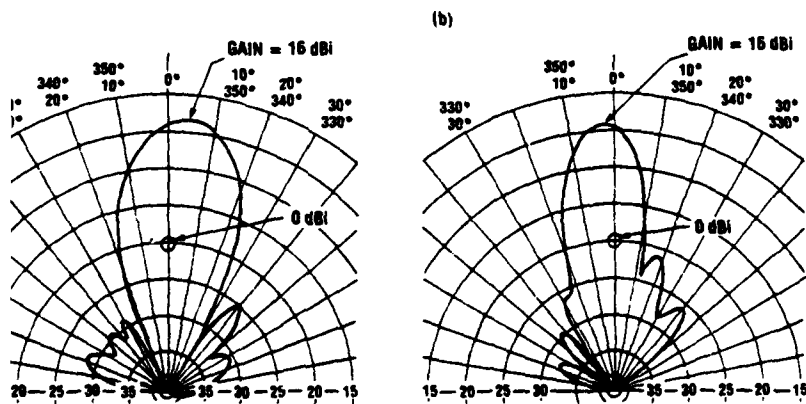


Fig. 9. Polar plots of antenna radiation patterns:
 (a) E-plane and (b) H-plane.

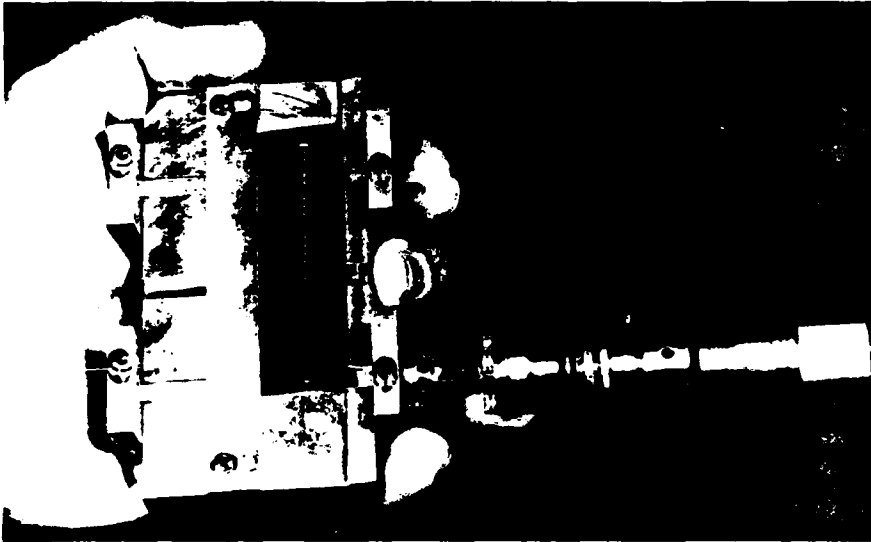


Fig. 10. Microstrip design of first U.S. Army near-millimeter wave antenna.

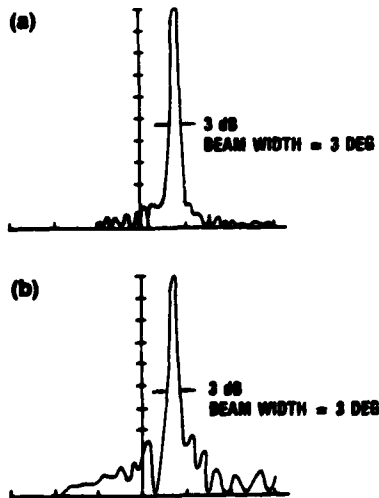


Fig. 11. Radiation patterns of first U.S. Army near-millimeter wave monolithic conformal antenna with linear phased array: (a) theory and (b) experiment.

CAMPI

Conclusions and Recommendations

By using a simple transmission line model of shunt conductance elements along with present computer programming techniques, linear array microstrip antennas can now be simulated, designed, and studied in a short time and at a low cost. Measurements of resonant frequency and beam angle of all the antennas fabricated show excellent correlation with the design data submitted to the computer. Cross polarization of the fields and mutual coupling of the array elements appear to be minimal. Several antennas etched by using the same negative have shown identical return-loss measurements and radiation patterns indicating excellent reproducibility.

Additional work is needed in obtaining a better analytical model and data on the element values of conductance and insertion phase as a function of patch width, characteristic impedance, and loading. When incorporated with an ABCD parameter and transmission matrix calculations, this approach should improve the antenna side-lobe levels and the overall measured design performance. Additional information must be gathered to better describe the radiation pattern and the directivity of a single patch element. Further, it would be desirable to design series arrays having elements of equal widths, but with different characteristic impedance lines interspaced between them. This design would provide for a simpler means of phase shifting the array since the insertion phase of each element is the same. Additionally, information about thick and low-loss substrates is needed so that arrays may be better designed to 100 GHz, where most of the commonly used dielectrics have thicknesses approaching the dimensions of one wavelength.

References

- (1) A. G. Derneryd IEEE Trans. Antennas Propag. AP-24, Nov 1976, 846-851.
- (2) I. G. Bahl and P. Bhartia, Microstrip Antennas, Artech House, Inc., 1980.
- (3) T. Metzler, Proc. Workshop on Printed Circuit Antenna Technology, New Mexico State Univ., Las Cruces, Oct 1979, pp 20/1-16.
- (4) P. P. Jedlicka and K. R. Carver, Proc. Workshop on Printed Circuit Antenna Technology, New Mexico State Univ., Las Cruces, Oct 1979, pp 4/1-19.
- (5) P. P. Jedlicka and K. R. Carver, IEEE Trans. Antennas Propag. AP-29, Jan 1981, 147-149.





